

1982

# Motion Analysis of Rolling Piston in Rotary Compressor

T. Yanagisawa

T. Shimizu

I. Chu

K. Ishijima

Follow this and additional works at: <https://docs.lib.purdue.edu/icec>

---

Yanagisawa, T.; Shimizu, T.; Chu, I.; and Ishijima, K., "Motion Analysis of Rolling Piston in Rotary Compressor" (1982). *International Compressor Engineering Conference*. Paper 392.  
<https://docs.lib.purdue.edu/icec/392>

This document has been made available through Purdue e-Pubs, a service of the Purdue University Libraries. Please contact [epubs@purdue.edu](mailto:epubs@purdue.edu) for additional information.

Complete proceedings may be acquired in print and on CD-ROM directly from the Ray W. Herrick Laboratories at <https://engineering.purdue.edu/Herrick/Events/orderlit.html>

# MOTION ANALYSIS OF ROLLING PISTON IN ROTARY COMPRESSOR

Tadashi Yanagisawa  
 Research Associate\*  
 Itsuo Chu  
 Senior Engineer\*\*

Takashi Shimizu  
 Professor\*  
 Kouji Ishijima  
 Engineer\*\*

\* Department of Mechanical Engineering, Shizuoka University, Hamamatsu, Japan.

\*\* Shizuoka Works, Mitsubishi Electric Corporation, Shizuoka, Japan.

## ABSTRACT

This paper is concerned with rolling piston type rotary compressor for air conditioner. rotating motion of the rolling piston is theoretically analysed using mathematical model which consists of dynamic equation of rolling piston, equation of force equilibrium and equation of bearing characteristic. Also the motion in operating compressor is measured by detecting the change of electrostatic capacity between rolling piston face and electrode mounted on cylinder head surface. After signal analysis, it is proved that rolling piston is sliding positive and negative alternately on the vane tip and it is rotating forward slowly around its center. Theoretical results are in good agreement with experimental results and the validity of the model is verified.

## INTRODUCTION

Rolling piston type rotary compressors are widely used for air conditioners. They have many advantages of small size, light weight, low cost and high performance as compared with reciprocating compressors. However, they also have disadvantages peculiar to the rotary compressors. One of these is friction loss which occurs closely related to motions of rolling piston (or roller) and vane (or blade) of the compressor.

In the past there have been some investigations to analyse motion of rolling piston and/or related friction loss [1-4]. However, most of them are analysing these by assuming steady state condition that rolling piston is rotating at average frequency and friction loss occurs under average loading. And the calculated results are not at all verified by experiment.

This paper attempts to analyse motion of rolling piston theoretically and experimentally. In theoretical analysis dynamic equation of rolling piston is solved with characteristic equations of finite length bearing. At experiment rotational motion of rolling piston in the operating compressor is measured using electrodes which detect electrostatic capacity. Theoretical results are verified by the comparison with experimental results.

## THEORETICAL ANALYSIS

### Dynamic Equation of Rolling Piston

Figure 1 shows schematic view of a rolling piston type rotary compressor. A rolling piston mounted on an eccentric of a shaft divides a cylinder room into two chambers, suction and compression chambers, associated with a vane. As the shaft rotates, the rolling piston rotates with the eccentric in the cylinder, which causes suction work in the suction chamber and compression and discharge work in the compression chamber.

There are many moments acting on the rolling piston. They are journal bearing moment  $M_c$  at the inner surface, vane tip moment  $r \times F_t$  at the outer surface, oil film moment  $M_b$  at the end faces.

Usually at the nearest point (A in Fig.1) between outer surface of rolling piston and inner surface of cylinder, some clearance exists and such moment that affects motion of rolling piston doesn't occur. Therefore, Dynamic equation of rolling piston around its center is expressed as follows.

$$I_p \dot{\omega}_p = M_c - r F_t - M_b \quad (1)$$

Each moment will be analysed in the following.

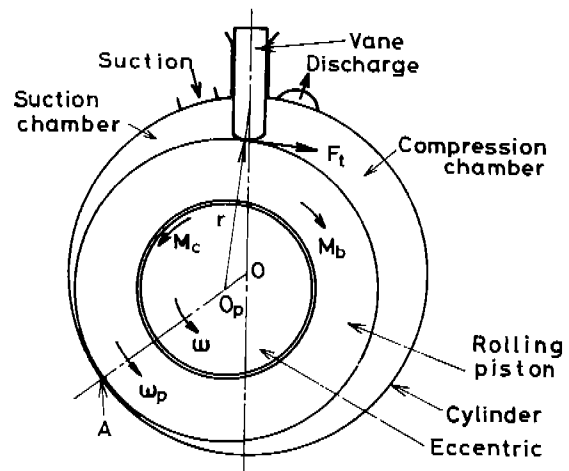


Fig. 1 Schematic view of rolling piston type rotary compressor

Analysis of Bearing Moment

The rolling piston and the eccentric constitute a kind of journal bearing. However, the rolling piston as bearing is rotating and bearing load is changing its magnitude and its direction. In this paper, the rolling piston bearing is analysed as an equivalent bearing shown in Fig. 2. Namely, the journal is rotating at the angular velocity of  $(\omega - \omega_p)$  and the bearing is not rotating. And direction of bearing load  $F$  is changing at the angular velocity of  $(\dot{\theta}_f - \omega_p)$ . Then, bearing moment  $M_c$  is given by next equation.

$$M_c = \frac{2\pi\eta(\omega - \omega_p) l_c r_c^3}{c\sqrt{1 - \epsilon^2}} - \frac{1}{2} c\epsilon F \sin\phi \quad (2)$$

Where, attitude  $\epsilon$  and attitude angle  $\phi$  of the bearing should be calculated based on theory of finite length bearing under dynamic loading. Here we use approximate calculating method developed by Nakagawa and Aoki [5,6]. According to that method, bearing pressure  $p$  is approximately expressed as follows.

$$p = \frac{24\eta \left(\frac{r_c}{c}\right)^2}{\pi} \frac{\sin(\pi z/l_c)}{(1 + \epsilon \cos\psi)^2} [\{\omega + \omega_p - 2(\dot{\theta}_f + \dot{\phi})\} \times (A_1 \sin\psi - A_2 \sin 2\psi + A_3 \sin 3\psi) + 2\dot{\epsilon} (C_0 - C_1 \cos\psi + C_2 \cos 2\psi - C_3 \cos 3\psi)] \quad (3)$$

Where,  $A_1 - A_3$  and  $C_0 - C_3$  are constant and function of bearing length ratio to diameter [5].

Balancing equation of oil film pressure and bearing load  $F$  is put down as follows.

$$\left. \begin{aligned} F \sin\phi &= \int_0^{l_c} \int_{\psi_1}^{\psi_2} p r_c \sin\psi \, d\psi \, dz \\ F \cos\phi &= -\int_0^{l_c} \int_{\psi_1}^{\psi_2} p r_c \cos\psi \, d\psi \, dz \end{aligned} \right\} \quad (4)$$

Where  $\psi_1$  and  $\psi_2$  are boundary angles of positive pressure region of oil film and they are the values

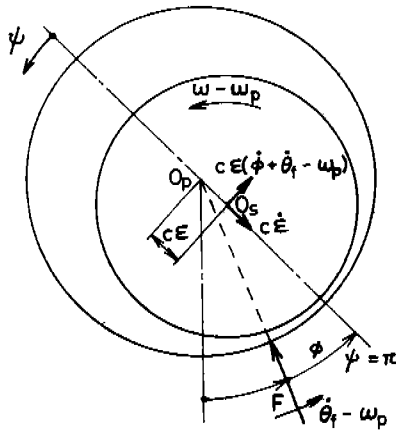


Fig. 2 Model of rolling piston bearing

of  $\psi$  which satisfy  $p=0$  at Eq.(3). Using these values Eq.(4) is represented as follows.

$$\left. \begin{aligned} F \sin\phi &= A\{\dot{\Phi}(A_1 I_{11} + A_2 I_{12} + A_3 I_{13}) \\ &\quad + 2\dot{\epsilon}(C_1 I_{21} + C_2 I_{22} + C_3 I_{23})\} \\ F \cos\phi &= A\{\dot{\Phi}(A_1 J_{11} + A_2 J_{12} + A_3 J_{13}) \\ &\quad + 2\dot{\epsilon}(C_1 J_{21} + C_2 J_{22} + C_3 J_{23})\} \end{aligned} \right\} \quad (5)$$

Where,  $A = \eta r_c l_c (r_c/c)^2 / \pi$ ,  $\Phi = \omega + \omega_p - 2(\dot{\theta}_f + \dot{\phi})$  and  $I_{11} \sim I_{23}$ ,  $J_{11} \sim J_{23}$  are functions of  $\epsilon$ ,  $\psi_1$  and  $\psi_2$  [5]. From Eq.(5) time differentials of attitude  $\epsilon$  and attitude angle  $\phi$  are given as follows.

$$\dot{\epsilon} = \frac{F(B_1 \cos\phi - B_3 \sin\phi)}{2A(B_1 B_4 - B_2 B_3)} \quad (6)$$

$$\dot{\phi} = \frac{1}{2}(\omega + \omega_p - 2\dot{\theta}_f) - \frac{F(B_4 \sin\phi - B_2 \cos\phi)}{2A(B_1 B_4 - B_2 B_3)} \quad (7)$$

Where  $B_1 = A_1 I_{11} + A_2 I_{12} + A_3 I_{13}$ ,  $B_2 = C_1 I_{21} + C_2 I_{22} + C_3 I_{23}$ ,  $B_3 = A_1 J_{11} + A_2 J_{12} + A_3 J_{13}$ ,  $B_4 = C_1 J_{21} + C_2 J_{22} + C_3 J_{23}$ .

$\epsilon$  and  $\phi$  are got by simultaneous integration of Eqs.(3), (6) and (7) numerically.

Analysis of Bearing Load

Figure 3 shows forces acting on the rolling piston, namely, gas compression force  $F_p$ , centrifugal force  $F_e$ , vane contact force  $F_n$  and  $F_t$ . Combined force of them becomes bearing load. Magnitude  $F$  and direction  $\theta_f$  of bearing load are expressed as follows when  $F_r$  and  $F_\theta$  are radial and angular components of bearing load given by Eqs.(10) and (11) respectively.

$$F = \sqrt{F_r^2 + F_\theta^2} \quad (8)$$

$$\theta_f = \theta + \tan^{-1}(F_\theta/F_r) \quad (9)$$

$$F_r = F_p \cos \frac{\theta + \alpha}{2} - F_n \cos(\theta + \alpha) - F_t \sin(\theta + \alpha) + F_e \quad (10)$$

$$F_\theta = -F_p \sin \frac{\theta + \alpha}{2} + F_n \sin(\theta + \alpha) - F_t \cos(\theta + \alpha) \quad (11)$$

In above equations, centrifugal force  $F_e$  and gas compression force  $F_p$  are evaluated as follows.

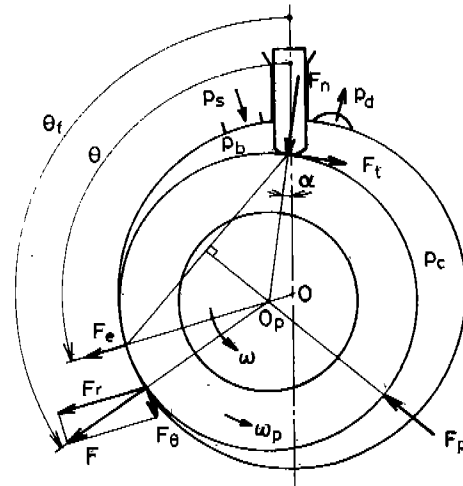


Fig. 3 Forces acting on rolling piston

$$F_e = m_p e \omega^2 \quad (12)$$

$$F_p = 2r\ell(p_c - p_b) \sin \frac{\theta + \alpha}{2} \quad (13)$$

Here, suction chamber pressure  $p_b$  is assumed to be constant and equal to suction pressure  $p_s$  of the compressor. And compression chamber pressure  $p_c$  is assumed to rise adiabatically till discharge valve opens (pressure  $p_d'$ , angle  $\theta_d$ ) and after that to decrease linearly with shaft rotational angle  $\theta$  as shown in Fig.4.

$$p_b = p_s \quad (14)$$

$$p_c = \begin{cases} p_s (V_s / V_c)^k & (\theta \leq \theta_d) \\ p_d + (p_d' - p_d) \frac{2\pi - \theta}{2\pi - \theta_d} & (\theta > \theta_d) \end{cases} \quad (15)$$

Where,  $V_s$  is suction volume and  $V_c$  is compression chamber volume expressed as follows.

$$V_s = \pi (R^2 - r^2) \ell + V_t \quad (16)$$

$$V_c = V_s - \frac{1}{2}r^2\ell\theta + \frac{1}{2}r^2\ell(\theta + \alpha) + \frac{1}{2}e\ell(r + r_v)\sin(\theta + \alpha) - \frac{1}{2}r_v^2\ell\tan\alpha - \frac{1}{2}b\ell x \quad (17)$$

#### Analysis of Forces acting on vane

Figure 5 shows forces acting on the vane, namely, contact forces  $F_t$  and  $F_n$  with rolling piston, contact forces  $R_1$ ,  $R_2$  and  $R_{t1}$ ,  $R_{t2}$  with vane slot,

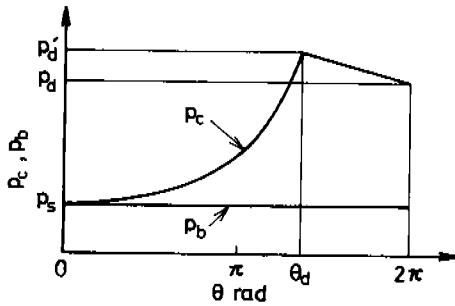


Fig. 4 Pressure - angle diagram

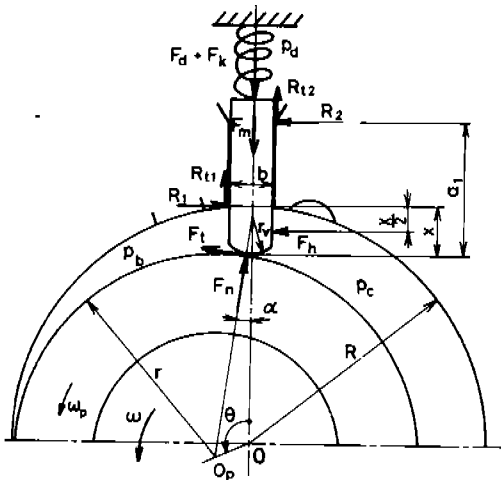


Fig. 5 Forces acting on vane

pressure differential force  $F_h$  across the vane within the cylinder, pressure differential force  $F_d$  in and out of cylinder, vane spring force  $F_k$  and inertial force  $F_m$ . Each force is expressed as follows.

$$F_h = x\ell(p_c - p_b) \quad (18)$$

$$F_d = \ell b p_d - \ell p_c (b/2 + r_v \sin\alpha) - \ell p_b (b/2 - r_v \sin\alpha) \quad (19)$$

$$F_k = k(x_0 - x) \quad (20)$$

$$F_m = -m_v \ddot{x} \quad (21)$$

Here, balancing equations of acting forces and moments are expressed as follows.

$$F_h + R_2 - R_1 + F_t \cos\alpha - F_n \sin\alpha = 0 \quad (22)$$

$$F_d + F_h + F_m - R_{t1} - R_{t2} - F_t \sin\alpha - F_n \cos\alpha = 0 \quad (23)$$

$$R_2 (a_1 - r_v + r_v \cos\alpha) - R_1 (x - r_v + r_v \cos\alpha) + F_h (x/2 - r_v + r_v \cos\alpha) + b (R_{t2} - R_{t1}) / 2 - r_v \sin\alpha (F_t \sin\alpha + F_n \cos\alpha) = 0 \quad (24)$$

At contact points, acting forces are assumed to have next relations as  $\mu_v$  is coefficient of friction at contact point with rolling piston and  $\mu_s$  is coefficient of friction at contact point with vane slot.

$$F_t = \mu_v F_n \quad (25)$$

$$R_{t1} = \mu_s R_1, \quad R_{t2} = \mu_s R_2 \quad (26)$$

From Eqs.(22) ~ (24), normal force  $F_n$  at vane tip is derived as follows.

$$F_n = \{ (F_d + F_k + F_m) (x - a_1) + \mu_v F_h (a_1 + b \mu_s) \} / [ (\cos\alpha + \mu_v \sin\alpha) (x - a_1 - 2\mu_s r_v \sin\alpha) + \mu_s (\sin\alpha - \mu_v \cos\alpha) \{ x + a_1 + b \mu_s - 2r_v (1 - \cos\alpha) \} ] \quad (27)$$

For  $\mu_v$  and  $\mu_s$ , experimental values will be used.

#### Oil Film Moment at Rolling Piston Faces

There exists oil film between rolling piston face and cylinder head surface. Its shearing force acts as braking moment on rotating rolling piston. By assuming, at each face, oil film thickness is equal to the half of total rolling piston face clearance  $\delta_b$ . The moment  $M_b$  at both faces is expressed as follows.

$$M_b = 2\pi r \omega_p (r^4 - r_c^4) / \delta_b \quad (28)$$

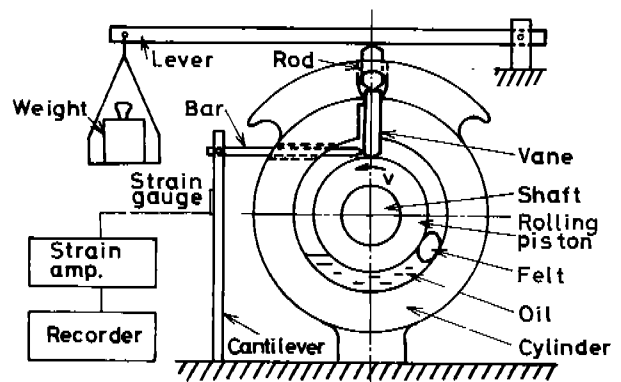


Fig. 6 Experimental apparatus to measure coefficient of friction at vane tip

EXPERIMENT

Measurement of Coefficient of Friction

Figure 6 shows experimental apparatus to measure coefficient of friction at contact point between vane tip and outer surface of rolling piston. Rolling piston is located at cylinder center and is rotating with shaft driven by a variable speed motor. While, vane is set in the vane slot loaded by the weight through lever and rod. Frictional force arisen at vane tip is transmitted to cantilever by the bar and measured by strain gauge on the cantilever. Lubricating condition is such that outer surface of rolling piston is wetted by the felt drenched with refrigerating oil. At experiment, loading weight and rotational frequency of rolling piston and temperature of lubricating oil are changed.

Figure 7 shows measuring apparatus of coefficient of friction at vane side. In the vane slot the vane is moving back and forth according to the oscillating motion of lever driven by cam shaft. While, horizontal force perpendicular to moving direction is loaded by spring balance. Frictional force between vane sides and vane slot is transmitted to lever through rod and measured by strain gauge on the lever. Lubricating condition is such that refrigerating oil is continuously poured from the top of the vane. At experiment, horizontal force and rotational frequency of cam shaft are changed.

Measurement of Rolling Piston Motion

Figure 8 shows a schematic view of an experimental compressor for measurement of rolling piston motion. Figure 9 shows cross section (A-A in Fig.8) of the compressor. On the rolling piston face, twelve small slot (1mm width  $\times$  1mm depth,  $\pi/6$  rad pitch) are radially digged by electrical discharge machining. On the other hand, on the frame (upper cylinder head) surface, electrically insulated three electrodes (1 mm dia.) are located on the pitch circle which overlaps every slot and their pitch angle is one third of the slot pitch angle.

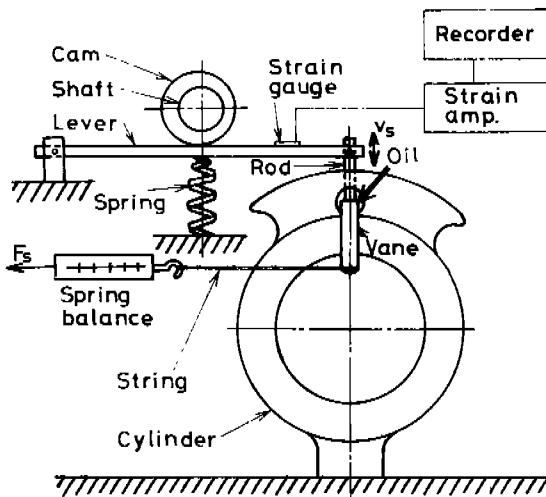


Fig. 7 Experimental apparatus to measure coefficient of friction at vane side

Rotating motion of rolling piston is caught by picking up the signals of electrostatic capacity between electrode and rolling piston face. By analysis of three signals from electrodes, not only average but also instantaneous rotation of rolling piston during one revolution of shaft become clear.

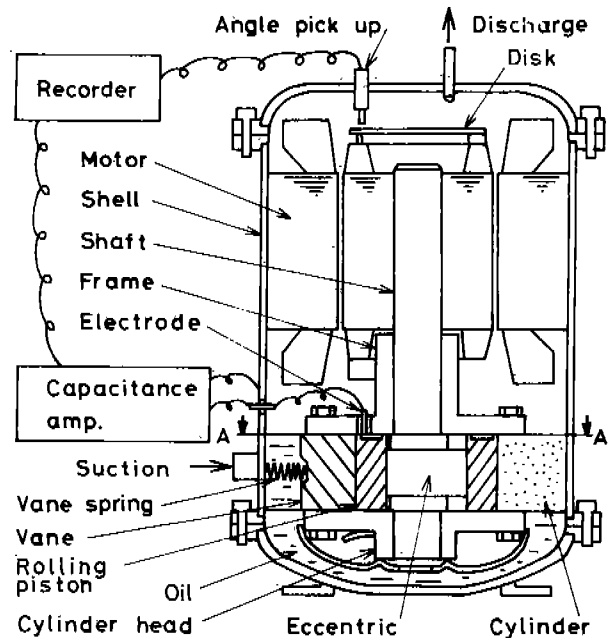


Fig. 8 Schematic view of experimental compressor

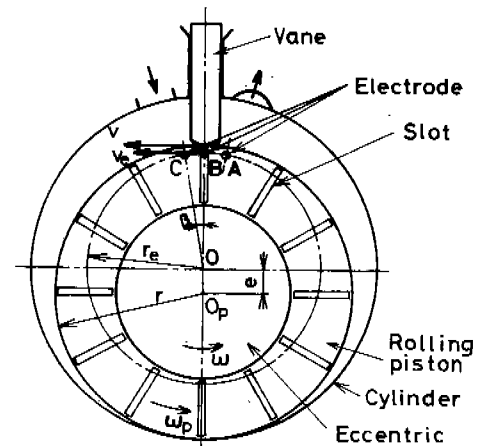


Fig. 9 Cross section (A-A in Fig.8) of the compressor

Table 1 Main dimensions of four designs of compressor used for experiment (dim. in mm)

Comp.	R	r	r <sub>c</sub>	r <sub>v</sub>	l	l <sub>e</sub>	a	b
1	27.0	24.3	14.4	6.0	23.8	14.0	24.0	4.7
2	27.0	21.8	15.7	6.0	30.8	21.0	24.0	4.7
3	29.0	25.5	17.5	6.0	50.0	32.0	26.0	4.7
4	29.0	23.3	17.5	6.0	50.0	32.0	26.0	4.7

Rotational angle of the shaft is detected by the eddy current type transducer which senses revolution of disk with teeth fixed on the motor rotor.

Experimental compressor is joined to refrigerating cycle used refrigerant R-22 as working fluid. The compressor is operated under given steady condition, and signals from rotating rolling piston and shaft are recorded by ultra-violet recorder. Table 1 shows main dimensions of four designs of compressor used for experiment.

By the way, in the case of compressors 2, 3 and 4 in Table 1, because of dimensional limitation, only average rotation of rolling piston is measured by using one electrode and one slot.

## RESULTS AND DISCUSSIONS

### Measured Results of coefficient of Friction

Figure 10 shows coefficient  $\mu_v$  of friction at vane tip.  $\mu_v$  is defined as  $F_t/F_n$ . Horizontal axis of the figure is expressed by dimensionless lubricating parameter  $\eta v/(F_n/l)$ . Not depending on experimental conditions,  $\mu_v$  is almost constant in the range of  $\eta v/(F_n/l)$  less than  $10^{-6}$ , where lubricating condition is considered to be boundary condition. On the other hand, in the range of larger  $\eta v/(F_n/l)$ ,  $\mu_v$  is decreasing with increase of  $\eta v/(F_n/l)$ , this means

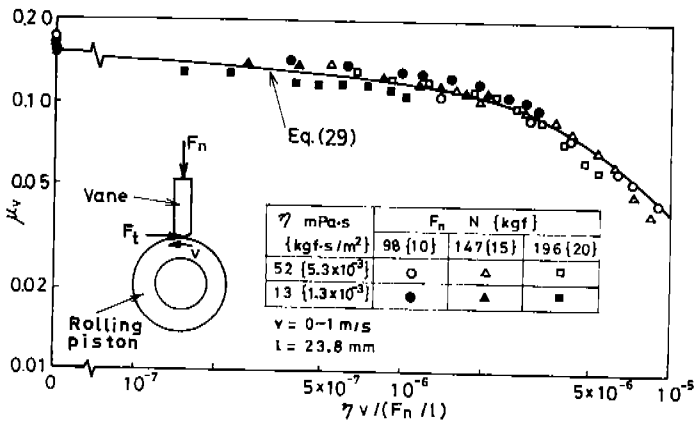


Fig. 10 Coefficient of friction at vane tip

mixed lubricating condition. In this paper  $\mu_v$  is approximated by next empirical formula.

$$\eta v = 0.15 \sim 35 \sqrt{\eta v / (F_n / l)} \quad (29)$$

In addition, measured  $\mu_v$  is not so much affected by the supplying condition of lubricating oil.

Figure 11 shows coefficient  $\mu_s$  of friction at vane side. By assuming that  $\mu_s$  at two contact points on both sides of vane are equal,  $\mu_s$  is calculated by next equation.

$$\mu_s = \frac{R_{t1}}{R_1} = \frac{R_{t2}}{R_2} = \frac{R_{t1} + R_{t2}}{R_1 + R_2} \quad (30)$$

Where, the denominator  $R_1 + R_2$  ( $\equiv R_{12}$ ) of the most right side of Eq.(30) is given by Eq.(31) taking account of moment balance of acting forces. While, the numerator  $R_{t1} + R_{t2}$  is evaluated by Eq.(32) compensating inertial force  $F_m$  of the vane.

$$R_{12} = F_s(2l_2 - l_1)/l_1 \quad (31)$$

$$R_{t1} + R_{t2} = F_l + F_m \quad (32)$$

In Fig.11, though  $\mu_s$  is a little scattered,  $\mu_s$  is considered to be constant in the wide range of dimensionless lubricating parameter  $\eta v_s/(R_{12}/l)$ . This means lubricating condition is almost boundary lubrication on the vane side. At the theoretical analysis,  $\mu_s$  is assumed to be constant and equal to 0.15.

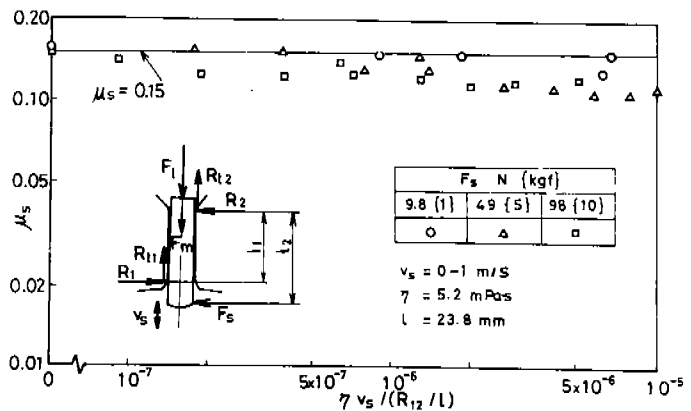


Fig. 11 Coefficient of friction at vane side

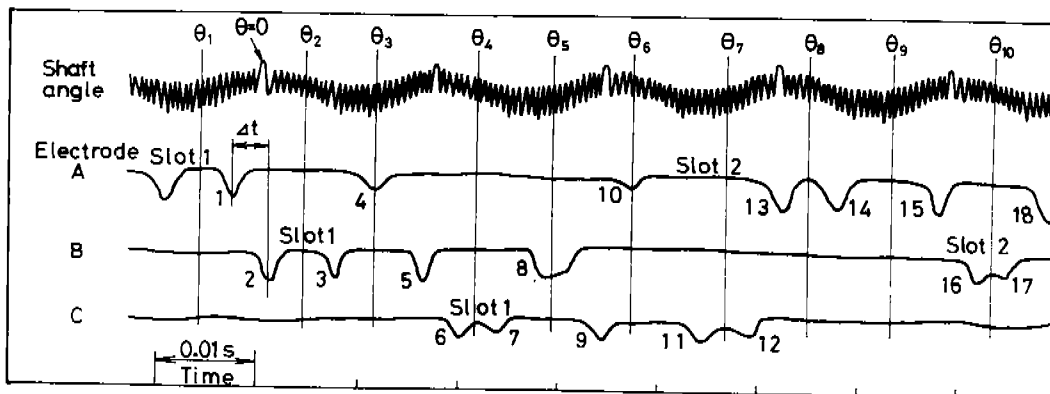


Fig. 12 Recorded chart of signals

### Signal Analysis of Rolling Piston Motion

Figure 12 shows an example of recorded chart. It includes slot passing signals from three electrodes A, B and C. Downward peak of the signal means that a slot passes by the position of an electrode. Also, the signal of shaft angle is included in Fig.12. Larger upward peak of the signal indicates shaft angle  $\theta=0$  rad.

Here, the location of rolling piston corresponding to  $\theta=\theta_1$  in Fig.12 is assumed to be as shown in Fig. 13(1) and the slot locating just before the electrode A is named slot 1. In Fig.12, slot passing peaks 1 and 2 are recorded in the order of electrode A and B. This means slot 1 has moved to the position between electrodes B and C. The location of rolling piston at  $\theta=\theta_2$  is considered to be as shown in Fig. 13(2). Then average velocity  $v_e$  of rolling piston at the place of electrodes is approximated by the next equation.

$$v_e = r_e \beta / \Delta t \quad (33)$$

Where,  $\Delta t$  is time difference between two peaks. Corresponding to  $v_e$ , angular velocity  $\omega_p$  of rolling piston and sliding velocity  $v$  at vane tip are calculated as follows.

$$\omega_p = (v_e - e\omega \cos\theta) / (r_e - e \cos\theta) \quad (34)$$

$$v = r\omega_p + e\omega \cos\theta / \cos\alpha \quad (35)$$

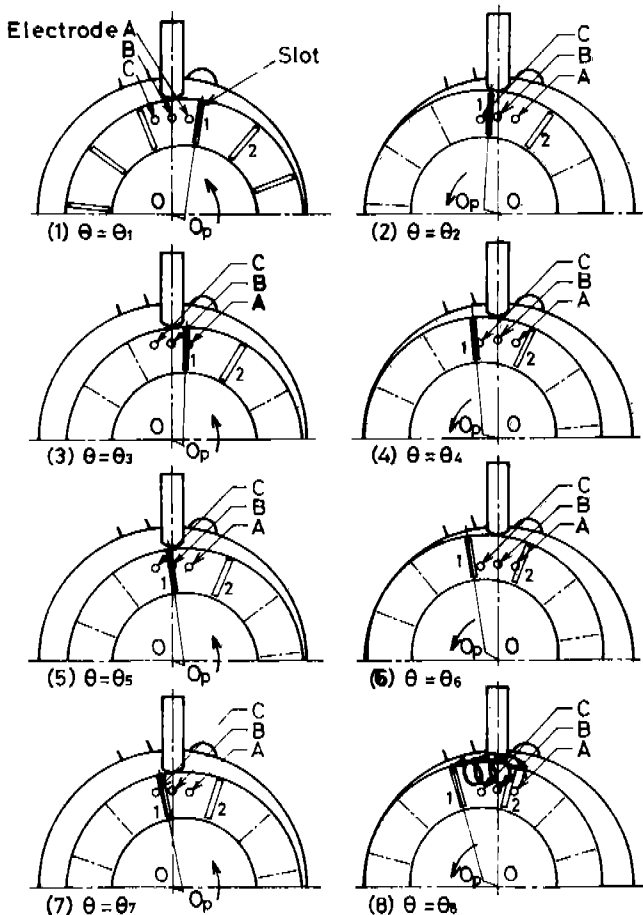


Fig. 13 Process of rolling piston motion

As slot passing peaks 3 and 4 are recorded in the order of electrodes B and A in Fig.12, rolling piston has moved backward during  $\theta=\theta_2 \sim \theta_3$ . Figure 13(3) shows location of rolling piston at  $\theta=\theta_3$ , just then slot 1 is overlapping with electrode A. Moreover, slot passing peaks 5 and 6 are recorded from electrodes B and C in Fig.12, which means slot 1 passes by position of electrode C as shown in Fig.13(4).

By analysis of signals shown in Fig.12 in the same manner, location of rolling piston corresponding to shaft angles  $\theta=\theta_5 \sim \theta_8$  are decided as shown Fig. 13(5) ~ (8). Slot passing peaks 10, 13 ~ 15 and 18 from electrode A are contributed by the slot 2. In Fig.13(8), locus of fixed point to slot 1 on the rolling piston is drawn from  $\theta=\theta_1$  to  $\theta=\theta_8$ . Rolling piston is revolving with its center and, as a whole, is rotating slowly around its center in the direction of shaft revolution.

### Discussion of Results

Experimental and theoretical results of motion analysis of rolling piston will be discussed in the following. Theoretical results are obtained by nume-

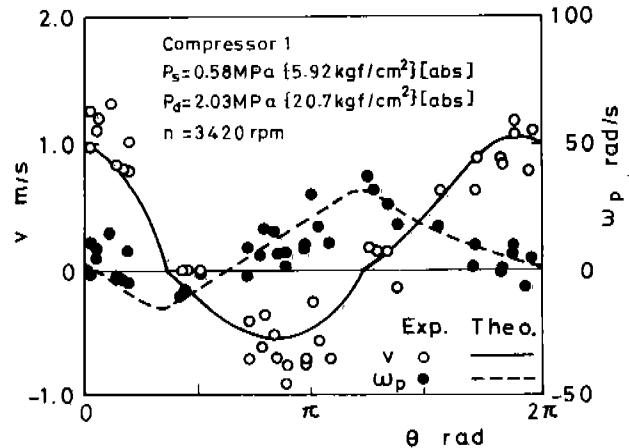


Fig. 14 Sliding velocity at vane tip and angular velocity of rolling piston (1)

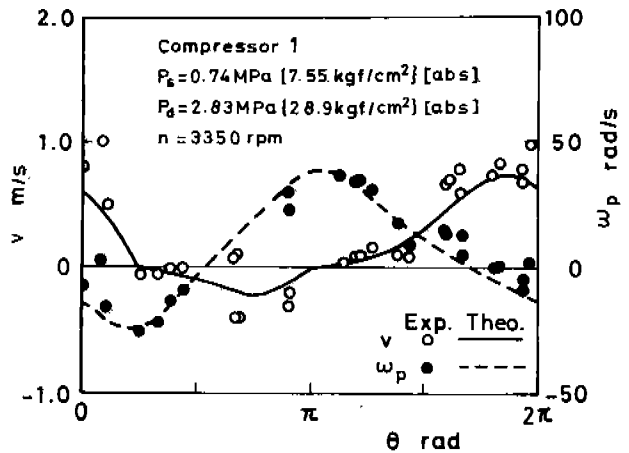


Fig. 15 Sliding velocity at vane tip and angular velocity of rolling piston (2)

rical calculation of Eqs.(1), (6), (7) using Runge-Kutta-Gill method. In that calculation, experimental coefficients of friction described before are used and viscosity of lubricating oil is rated taking account of solubility of refrigerant under operating pressure and temperature.

Figure 14 shows sliding velocity  $v$  at vane tip and angular velocity  $\omega_p$  of rolling piston during one revolution of the shaft.  $v$  is positive in the neighbourhood of  $\theta=0$  ( $2\pi$ ) rad, which means rolling piston is sliding toward shaft revolution at vane tip. But in the neighbourhood of  $\theta=\pi$  rad,  $v$  is negative, namely, rolling piston is sliding against shaft revolution.

On the other hand,  $\omega_p$  is changing between positive and negative according to the change of  $v$ . But the maximum absolute value of  $\omega_p$  is less than one tenth of shaft angular velocity ( $\omega=360$  rad/s). Therefore, at the right side of Eq.(35), the second term, which is sliding component based on revolving motion of rolling piston center around shaft center, is more influential on sliding velocity than the first term, which is the sliding component based on rotational motion of rolling piston around its center. In the neighbourhood of  $\theta=\pi$ , the second term becomes negative and  $v$  becomes negative, namely, backward sliding occurs at the vane tip.

Though experimental results shown in Fig.14 are a little scattered, they agree fairly well with theoretical results.

Figure 15 shows experimental and theoretical results when the compressor is operated with higher load than that in the case of Fig.14. Absolute value of  $v$  is less but amplitude of  $\omega_p$  is larger as compared with those in Fig.14.

The decrease of sliding velocity means that, with increase of pressures, the increase of braking moment at vane tip is larger than the increase of driving moment at rolling piston bearing. In this case, theoretically calculated results are in good agreement with experimental results.

Table 2 shows list of average rotational frequency

Table 2 Comparison of experimental and theoretical results

Comp.	Operating condition			R. piston freq.	
	Pressur (abs.)		Freq. n rpm	$n_p$ rpm	
	$P_s$ MPa	$P_d$ MPa		Exp.	Theo.
1	0.58	2.03	3420	64	77
	0.58	2.03	2880	62	56
	0.74	2.83	3350	63	54
2	0.58	2.03	3400	142	157
	0.58	2.03	2850	51	47
	0.72	2.53	3350	48	46
3	0.58	2.03	3450	132	131
	0.58	2.03	2880	49	67
4	0.58	2.03	3450	161	158
	0.58	2.03	2880	32	32
	0.72	2.53	3400	73	63

1 MPa = 10.2 kgf/cm<sup>2</sup>

$n_p$  of rolling piston for four designs of compressor under several operating conditions. As a whole,  $n_p$  is a few percentages of rotational frequency  $n$  of shaft. At the same compressor,  $n_p$  decreases with decrease of  $n$  and with increase of pressures. Under the same operating condition,  $n_p$  is different for each compressor design. As a whole, theoretical results agree fairly well with experimental results.

It is verified that theoretical calculation derived in this paper is valid to analyse rolling piston motion and to estimate the effects of operating parameter and design parameter of the compressor.

#### An Example of Friction Loss

Figure 16 shows an example of friction losses related to rolling piston motion and peculiar to this type compressor. Vane tip loss  $L_v$ , vane side loss  $L_s$  and rolling piston bearing loss  $L_c$  are derived from next equations.

$$L_v = v F_t \quad (36)$$

$$L_s = (R_{t1} + R_{t2}) \dot{x} \quad (37)$$

$$L_c = \omega M_c \quad (38)$$

They can be easily calculated by using loss components resulted from motion analysis of rolling piston. Losses are waving during one revolution of the shaft affected by the rolling piston motion. In this case average of total loss  $L_t$  reaches about 7 % of average gas compression power of the compressor.

#### CONCLUSION

In this paper, motion of rolling piston in rotary compressor for air conditioner was analysed theoretically and experimentally.

It was proved that positive and negative sliding between vane tip and outer surface of rolling piston is occurring alternately during one revolution of shaft and rolling piston is rotating at average rotational frequency of a few percentages of shaft frequency. Rotational frequency of rolling piston decreased with decrease of shaft frequency and with increase of compressor load. Theoretical results using approximate theory of finite length bearing and empirical coefficients of friction agreed fairly well with experimental results and the validity of the theoretical analysis was verified.

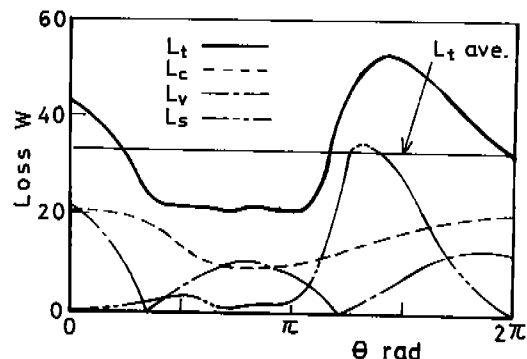


Fig. 16 Friction losses



## NOMENCLATURE

$\alpha$  = vane length  
 $a_1$  = distance between vane tip and reaction point  
 $b$  = vane thickness  
 $c$  = radial clearance at rolling piston bearing  
 $e$  = eccentricity of eccentric =  $R-r$   
 $F$  = bearing load  
 $F_d$  = pressure differential force across vane within cylinder  
 $F_e$  = centrifugal force of rolling piston  
 $F_h$  = pressure differential force across vane in and out of cylinder  
 $F_k$  = vane spring force  
 $F_l$  = force of cantilever  
 $F_m$  = inertial force of vane  
 $F_n, F_t$  = normal and tangential force at vane tip  
 $F_p$  = gas compression force of rolling piston  
 $F_r, F_\theta$  = radial and angular components of bearing load  
 $F_s$  = force of spring balance  
 $I_p$  = moment of inertia of rolling piston  
 $L_c$  = friction loss at rolling piston bearing  
 $L_s$  = friction loss at vane side  
 $L_t$  = total friction loss =  $L_c + L_s + L_v$   
 $L_v$  = friction loss at vane tip  
 $l$  = cylinder length  
 $l_c$  = eccentric length (=bearing length)  
 $l_1, l_2$  = distances between force acting points  
 $M_b$  = friction moment at rolling piston face  
 $M_c$  = friction moment at rolling piston bearing  
 $m_p$  = mass of rolling piston  
 $m_v$  = mass of vane  
 $n$  = rotational frequency of shaft  
 $n_p$  = rotational frequency of rolling piston  
 $p$  = pressure  
 $p_b, p_c$  = pressures in suction and compression chambers  
 $p_s, p_d$  = suction and discharge pressures of compressor  
 $R$  = cylinder radius  
 $R_{t1}, R_{t2}$  = tangential forces at vane side contact points  
 $R_1, R_2$  = normal forces at vane side contact points  
 $R_{12} = R_1 + R_2$   
 $r$  = rolling piston outer radius  
 $r_c$  = eccentric radius (=bearing radius)  
 $r_e$  = pitch circle radius of electrodes  
 $r_v$  = vane tip radius  
 $\Delta t$  = time difference between signals

$V_c$  = compression chamber volume  
 $V_s$  = suction volume  
 $V_t$  = clearance volume  
 $v$  = sliding velocity at vane tip  
 $v_e$  = average velocity of slot  
 $v_s$  = sliding velocity at vane side  
 $x$  = vane extension =  $R + r_v - (r + r_v) \cos \alpha - e \cos \theta$   
 $x_0$  = initial deflection of vane spring  
 $z$  = coordinate of bearing length  
 $\alpha$  = offset angle of rolling piston center =  $\sin^{-1} \{e / (r + r_v) \times \sin \theta\}$   
 $\beta$  = pitch angle of electrode  
 $\delta b$  = total clearance on rolling piston faces  
 $\epsilon$  = attitude of bearing  
 $\eta$  = viscosity of lubricating oil  
 $\theta$  = rotational angle of shaft  
 $\theta_f$  = directional angle of bearing load  
 $\kappa$  = adiabatic exponent  
 $\mu_s$  = coefficient of friction at vane side  
 $\mu_v$  = coefficient of friction at vane tip  
 $\phi$  = attitude angle of bearing  
 $\psi$  = coordinate of bearing angle  
 $\omega$  = angular velocity of shaft  
 $\omega_p$  = angular velocity of rolling piston  
 $\cdot$  = time differential

## REFERENCES

- 1 Okada, K., and Kuyama, K., "Analysis on Planetary Motion of the Rolling Piston in a Rotary Compressor (Theoretical Analysis of Mechanical Friction)," (in Japanese), Refrig., Japan. Vol.50 No.571, 1975. pp.331-337.
- 2 Pandeya, P., and Soedel, W., "Rolling Piston Type Rotary Compressors with Special Attention to Friction and Leakage," Proc. Purdue Compressor Tech. Conf., 1978, pp.209-218.
- 3 Chu, I., et al., "Analysis of the Rolling-Piston type Rotary Compressor," Proc. Purdue Compressor Tech. Conf., 1978, pp.219-224.
- 4 Ozu, M., and Itami, T., "Efficiency Analysis of Power Consumption in Small Hermetic Refrigeration Rotary Compressors," Int. J. Refrig., Vol.4 No.5, 1981, pp.265-270.
- 5 Nakagawa, E., and Aoki, H., "Dynamic Characteristics of Rotor - Bearing System Supported by Journal Bearings," (in Japanese), Lubrication, Japan, Vol.13 No.3, 1968, pp.117-125.
- 6 Nakagawa, E., and Aoki, H., "A Calculation Method of Characteristic Performance of Journal Bearings Under Dynamic Loading," (in Japanese), Lubrication, Japan, Vol.15 No.7, 1970, pp.385-390.